Int J Clin Exp Pathol 2020;13(10):2455-2473
www.ijcep.com /ISSN:1936-2625/IJCEP0106437

Original Article

Long non-coding RNA MAFG-AS1 knockdown blocks malignant progression in breast cancer cells by inactivating JAK2/STAT3 signaling pathway via MAFG-AS1/miR-3196/TFAP2A axis

Mingxing Ding[1], Yongqiang Fu[1], Fangming Guo[1], Haohao Chen[1], Xiaoyan Fu[1], Wenzhuang Tan[1], Hui Zhang[2]

[1]*Medical Molecular Biology Laboratory, Medical College, Jinhua Polytechnic, Jinhua, Zhejiang, China;* [2]*Department of Laboratory Animals Center, Jinhua Institute for Food and Drug Control, Jinhua, Zhejiang, China*

Received December 15, 2019; Accepted January 19, 2020; Epub October 1, 2020; Published October 15, 2020

Abstract: Background: Breast cancer is still a leading threat to women's lives. Long non-coding RNAs (lncRNA) associated with cancer progression are getting attention. The objective of this study was to investigate the role of lncRNA MAFG-antisense 1 (MAFG-AS1) and mechanisms of action in breast cancer. Methods: The expression of MAFG-AS1, microRNA-3196 (miR-3196) and transcription factor AP-2 alpha (TFAP2A) was detected by quantitative real-time polymerase chain reaction (qRT-PCR). The cell proliferation was assessed by 3-(4, 5-dimethyl-2-thiazolyl)-2, 5-diphenyl-2-H-tetrazolium bromide (MTT) assay. The number of colonies was observed through colony formation assay. The protein levels of Cyclin D1, Ki67, Bcl-2 associated X protein (Bax), B-cell lymphoma2 (Bcl-2), Hexokinase II (HK2), lactate dehydrogenase A (LDHA), TFAP2A, Janus kinase 2 (JAK2), phosphorylated-JAK2 (p-JAK2), signal transducer and activator of transcription 3 (STAT3), and phosphorylated-STAT3 were quantified by western blot. The cell apoptosis was monitored using flow cytometry. The glycolysis progression was evaluated according to glucose consumption and lactate production. The relationship between miR-3196 and MAFG-AS1 or TFAP2A was predicted by the online tool starBase and verified by the dual-luciferase reporter assay. The role of MAFG-AS1 *in vivo* was determined by the tumor formation assay in nude mice. Results: MAFG-AS1 was highly expressed in tumor tissues and cells. MAFG-AS1 knockdown restrained proliferation, colony formation, and glycolysis but promoted apoptosis of breast cancer cells. MiR-3196 was a target of MAFG-AS1, and its inhibition reversed the role of MAFG-AS1 knockdown. TFAP2A was a target of miR-3196, and its overexpression abolished the effects of miR-3196 reintroduction. MAFG-AS1 knockdown suppressed the activity of the JAK2/STAT3 signaling pathway. Moreover, MAFG-AS1 knockdown reduced tumor growth *in vivo*. Conclusion: MAFG-AS1 knockdown attenuated breast cancer progression *in vitro* and *in vivo* through activation of the JAK2/STAT3 signaling pathway by the MAFG-AS1/miR-3196/TFAP2A regulatory axis.

Keywords: MAFG-AS1, miR-3196, TFAP2A, breast cancer, JAK2/STAT3

Introduction

Breast cancer is the most commonly diagnosed cancer in women worldwide and the second leading cause of cancer-related death [25]. According to statistics, over 1,675,000 women are diagnosed with breast cancer each year, and over 500,000 women die of this cancer [8]. Breast cancer is a highly heterogeneous, pathogenic, and complex disease [20]. Although advances in early detection and cancer treatment have led to a reduction of mortality, breast cancer remains a significant public concern problem with an unsatisfactory prognosis [15, 22]. Therefore, understanding the molecular mechanisms resulting in the development of breast cancer remains the mainstay of improved diagnosis and treatment. It is urgent to identify novel biomarkers associated with tumorigenesis to elucidate the molecular mechanisms of breast cancer processes.

Previous work summarized that long non-coding RNAs (lncRNAs) and microRNAs (miRNAs) might play crucial roles in the development of numerous human cancers, including breast cancer, and could be novel biomarkers for future treatment [1, 2, 10]. LncRNAs are novel

RNAs with >200 nucleotides and play their roles by modulating various biologic processes, including cell proliferation, differentiation, glycolysis and invasion [26]. In breast cancer, several lncRNAs had been identified to participate in the progression of cancer, such as NDRG1-OT1, AGAP2-AS1 and 91H [6, 27, 35], providing novel insights into the mechanism of breast cancer development. LncRNA MAFG-antisense 1 (MAFG-AS1) was also mentioned to be associated with the aggressive progression of breast cancer, and carcinogenesis [13]. However, the study of MAFG-AS1 in breast cancer is still lacking, and the understanding of its role is still insufficient due to the limited mechanisms of action. Therefore, we explored novel mechanisms of action of MAFG-AS1 in breast cancer.

MiRNAs are a cluster of RNA molecules that regulate gene expression at the post-transcriptional level generally by interacting with the 3'untranslated region (3'UTR) of target mRNAs [17]. Aberrant expression of miRNAs involved in cancer development is considered to be a suitable entry point to explore the mechanism of cancer progression [31]. With the boom insequencing techniques, an increasing number of miRNAs is gradually detected and their functions are readily identified [31]. In breast cancer, dozens of miRNAs were confirmed to be linked to the cancer progression, such as miR-1287-5p, miR-153 and miR-30 [3, 14, 24]. Interestingly, a study discovered that miR-3196 was weakly expressed in breast tumor tissues with lymph node metastasis relative to non-lymph node metastasis [28]. Besides, another paper showed that miR-3196 overexpression inhibited cell proliferation in breast cancer cells [12]. We speculate that miR-3196 is a tumor suppressor at least in breast cancer and attempted to show a mechanism of action of miR-3196.

Transcription factor AP-2 alpha (TFAP2A) was reported to function in diverse cancers, such as neuroblastoma, bladder cancer, and breast cancer [5, 16, 23]. The data indicate that TFAP2A is a broadly expressed modulator in different types of cancer by acting as an oncogene to contribute to the cell growth, survival and metastasis in cancer. Here, we explore a novel mechanism associated with TFAP2A in breast cancer.

In our present study, the expression of MAFG-AS1 was investigated in breast cancer tissues and cells. Potential biologic functions of MAFG-AS1 were explored as well as the underlying action mechanism. The aim of this study was to broaden new insights into the role of MAFG-AS1 and provide an efficient biomarker for the treatment of breast cancer.

Materials and methods

Tissues

A total of 30 pairs of tumor tissues and adjacent normal tissues from breast cancer patients recruited from The Affiliated Hospital of Jinhua Polytechnic were collected and stored at -80°C until use. Every patient had signed informed consent prior to the operation. This study was approved by the Ethics Committee of Medical College, Jinhua Polytechnic.

Cell lines and cell culture

Breast cancer cell lines, including T47D, HCC-1937, MDA-MB-231 and MCF-7, and normal breast epithelial cell line MCF-10A were all purchased from KeyGen Biotech (Nanjing, China). MDA-MB-231 and MCF-7 cells were cultured in 90% Dulbecco's Modified Eagle Medium (DMEM; Gibco, Grand Island, NY, USA) containing 10% fetal bovine serum (FBS; Gibco). T47D, HCC1937 and MCF-10A cells were cultured in 90% Roswell Park Memorial Institute 1640 (RPMI 1640; Gibco) containing 10% FBS (Gibco). All cells were maintained at 37°C in a humidified atmosphere with 5% CO_2.

Quantitative real-time polymerase chain reaction (qRT-PCR)

Total RNA was isolated using TRIzol reagent (Invitrogen, Carlsbad, CA, USA). The RNA quality was checked with 1% agarose gel electrophoresis under ChemiDoc XRS system (Bio-Rad, Hercules, CA, USA) and detected using Nanodrop2000 (Thermo Fisher Scientific, Waltham, MA, USA). Subsequently, the RNA was reverse-transcribed into complementary DNA (cDNA) using the riboSCRIPT Reverse Transcription Kit (Ribobio, Guangzhou, China). The qRT-PCR reaction was conducted under CFX96 System (Bio-Rad) using SYBR Green Master PCR mix (Invitrogen). Changes in expression levels relative to reference genes (β-actin or U6) were calculated using the $2^{-\Delta\Delta ct}$ method. The primers used in qRT-PCR are shown as below:

MAFG-AS1: 5'-ATGACGACCCCCAATAAAGGA-3' (Forward) and 5'-CACCGACATGGTTACCAGC-3' (Reverse); miR-3196: 5'-CCTGTGTATGCATCCTCGACTG-3' (Forward) and 5'-CTGGCGTGTAATGGAGTCG-3' (Reverse); TFAP2A: 5'-TGCTACACTGAGACTCCCGT-3' (Forward) and 5'-GAATGCCTGGAAATCGAGCG-3' (Reverse); β-actin: 5'-GCTTCTAGGCGGACTGTTAC-3' (Forward) and 5'-CCATGCCAATGTTGTCTCTT-3' (Reverse); U6: 5'-CTCGCTTCGGCAGCACA-3' (Forward) and 5'-AACGCTTCACGAATTTGCGT-3' (Reverse).

Cell transfection

Small interfering RNAs against MAFG-AS1 (si-MAFG-AS1) and negative control (si-NC) were synthesized by Sangon Biotech (Shanghai, China). The mimics of miR-3196 (miR-3196), the inhibitor of miR-3196 (anti-miR-3196) and respective negative control (miR-NC or anti-miR-NC) were purchased from Ribobio. The vector pcDNA3.1-TFAP2A (pcDNA-TFAP2A) for the overexpression of PDK4 and the control pcDNA empty vector (pcDNA) were constructed by Sangon Biotech. Lentiviral vector (Lenti-short hairpin) for stable MAFG-AS1 downregulation (sh-MAFG-AS1) and corresponding negative control (sh-NC) were assembled by Genechem (Shanghai, China). Lipofectamine 3000 (Invitrogen) was utilized to conduct cell transfection.

3-(4, 5-dimethyl-2-thiazolyl)-2, 5-diphenyl-2-H-tetrazolium bromide (MTT) assay

T47D and MDA-MB-231 cells with separatetransfection were seeded into 96-well (5×10^3 cells per well) plates (Corning Costar, Corning, NY, USA). Then 10 μL MTT solution (Beyotime, Shanghai, China) was pipetted into each well at the indicated time points (0 h, 24 h, 48 h and 72 h) for 4 h at 37°C. After that, dimethyl sulfoxide (DMSO; Beyotime) was added into each well to dissolve the formazan. The absorbance was measured at 490 nm using the Multiskan Ascent (Thermo Fisher Scientific) to assess cell proliferation.

Colony formation assay

T47D and MDA-MB-231 cells with different transfection were digested with trypsin and seeded into 6-well (5×10^3 cells per well) plates (Corning Costar) for 2 weeks. Afterwards, cells were fixed with methanol and stained with 0.1% crystal violet for 20 min. Next, the number of colonies was observed bya microscope (Olympus, Tokyo, Japan) and counted using ImageJ software.

Western blot

Western blot was carried out according to the previous method [30]. Briefly, separated proteins were transferred onto the polyvinylidene fluoride (PVDF) membranes (Bio-Rad) and probed with primary antibodies against Cyclin D1 (ab16663; 1:200; Abcam, Cambridge, MA. USA), Ki67 (ab16667; 1:1000; Abcam), Bcl-2 associated X protein (Bax) (ab32503; 1:1000; Abcam), B-cell lymphoma2 (Bcl-2) (ab185002; 1:1000; Abcam), Hexokinase II (HK2) (ab22-7198; 1:5000; Abcam), lactate dehydrogenase A (LDHA) (ab125683; 1:1000; Abcam), TFAP2A (ab108311; 1:1000; Abcam), janus kinase 2 (JAK2) (ab108596; 1:5000; Abcam), phosphorylated-JAK2 (p-JAK2) (ab32101; 1:2000; Abcam), signal transducer and activator of transcription 3 (STAT3) (ab68153; 1:1000; Abcam), phosphorylated-STAT3 (ab76315; 1:2000; Abcam), β-actin (ab8227; 1:5000; Abcam) and goat anti-rabbit secondary antibodies (ab20-5718; 1:5000; Abcam). The protein signals were determined using the enhanced chemiluminescent reagent (Beyotime) through an imaging system (Bio-Rad).

Flow cytometry assay

The transfected T47D and MDA-MB-231 cells were seeded into 6-well plates to which was added 0.25% trypsin. After washing with phosphate buffer saline (PBS), the cells were resuspended by 500 μL binding buffer and incubated by 5 μL Annexin V-fluorescein isothiocyanate (FITC) and propidium iodide (PI) using the Annexin V-FITC Apoptosis Detection Kit (KeyGen Biotech), lasting for 15 min without light. Finally, the apoptotic cells were sorted using flow cytometer (BD Biosciences, San Jose, CA, USA).

Glycolysis analysis

Glycolysis progression was evaluated according to glucose consumption and lactate production. The glucose consumption and lactate production were investigated using a Glucose Assay Kit (Biovision; Milpitas, CA, USA) and Lactate Assay Kit (Biovision) in line with the product's instructions.

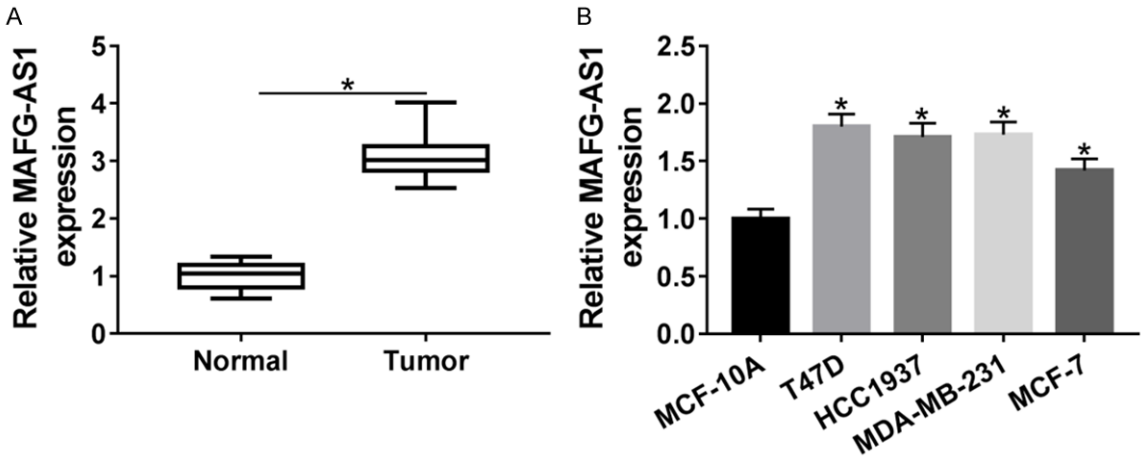

Figure 1. MAFG-AS1 is upregulated in breast cancer tissues and cells. A. The expression of MAFG-AS1 in tumor tissues (n=30) and normal tissues (n=30) was detected by qRT-PCR. B. The expression of MAFG-AS1 in breast cancer cell lines (T47D, HCC1937, MDA-MB-231 and MCF-7) and a normal breast epithelial cell line (MCF-10A) was detected by qRT-PCR. *$P < 0.05$.

Bioinformatics analysis

The Online database starBase (http://starbase.sysu.edu.cn/) was used to predict the potential target genes of lncRNA or miRNA and corresponding specific binding sites.

Dual-luciferase reporter assay

The fusion plasmids (pGL4, Promega, Madison, WI, USA) containing the wild-type sequences of MAFG-AS1 (MAFG-AS1-WT) harboring the binding sites with miR-15a-5p, the wild-type sequences of TFAP2A 3'UTR (TFAP2A 3'UTR-WT) harboring the binding sites with miR-15a-5p and their corresponding mutant-type sequences harboring the mutated binding sites with miR-15a-5p (MAFG-AS1-MUT and TFAP2A 3'UTR-MUT) were obtained from Sangon Biotech. Afterwards, the T47D and MDA-MB-231 cells were cotransfected with MAFG-AS1-WT, MAFG-AS1-MUT, TFAP2A 3'UTR-WT or TFAP2A 3'UTR-MUT and miR-3196 or miR-NC, respectively. The luciferase activity was determined using the Dual-Luciferase Reporter Assay Kit (Promega) at 48 h post-transfection.

Tumor formation assay in nude mice in vivo

All animal procedures were approved by the Animal Care and Use Committee of Medical College, Jinhua Polytechnic. Ten BALB/c nude mice (6-week-old, female) were purchased from HFK bioscience Co., LTD (Beijing, China). T47D cells with the transfection of sh-MAFG-AS1 or sh-NC were subcutaneously injected into the right flank of mice. Seven days after inoculation, the tumor volume was measured once a week based on the formula: length × width^2 × 0.5. Afterwards, the mice were killed after 35 days, and the tumor tissues were collected for the following analyses.

Statistical analysis

The data were collected from at least three repeated, independent experiments, analyzed by GraphPad Prism 5.01 (GraphPad Software, Inc., La Jolla, CA, USA) and presented as the mean ± standard deviation (SD). The differences were analyzed by Student's *t*-test or one-way analysis of variance (ANOVA) with post hoc LSD tests. The correlation analysis was investigated according to the Spearman's correlation coefficient. $P < 0.05$ was considered a significant difference.

Result

MAFG-AS1 was upregulated in breast cancer tissues and cell lines

The expression of MAFG-AS1 in breast cancer tissues and cell lines was detected to observe whether MAFG-AS1 was abnormally regulated. Noticeably, the expression of MAFG-AS1 was increased in tumor tissues (n=30) relative to adjacent normal tissues (n=30) (**Figure 1A**). Likewise, the expression of MAFG-AS1 was significantly enhanced in breast cancer cell lines, including T47D, HCC1937, MDA-MB-231, and

MCF-7, compared with that in human non-tumorigenic breast epithelial cell line MCF-10A (**Figure 1B**). Moreover, the expression of the MAFG-AS1 in T47D and MDA-MB-231 cell lines was greater than that in HCC1937 and MCF-7 cell lines. Therefore, T47D and MDA-MB-231 cells were chosen for the subsequent experiments. The data suggested that MAFG-AS1 was aberrantly upregulated in breast cancer tissues and cell lines.

MAFG-AS1 knockdown inhibited the malignant progression of breast cancer cells

The expression of MAFG-AS1 was knocked down in T47D and MDA-MB-231 cells by transfecting with si-MAFG-AS1 to investigate the role of MAFG-AS1 *in vitro*. First, the transfection efficiency was examined, and the result showed that the expression of MAFG-AS1 in T47D and MDA-MB-231 cells with si-MAFG-AS1 in different lines was notably decreased. Its expression most significantly decreased in the si-MAFG-AS1#3 group (**Figure 2A**). Hence, T47D and MDA-MB-231 cells transfected with si-MAFG-AS1#3 were used for the following analyses. MTT assay manifested that the proliferation in T47D and MDA-MB-231 cells transfected with si-MAFG-AS1#3 was prominently suppressed compared with si-NC (**Figure 2B** and **2C**). Then, a colony formation assay detected that MAFG-AS1 knockdown pronouncedly reduced the number of colonies of T47D and MDA-MB-231 cells (**Figure 2D**). Likewise, the protein levels of cell cycle regulator and cell proliferation marker, including Cyclin D1 and Ki67, were quantified, and the result displayed that the levels of Cyclin D1 and Ki67 were obviously declined in T47D and MDA-MB-231 cells transfected with si-MAFG-AS1#3 compared with si-NC (**Figure 2E** and **2F**). In addition, flow cytometry assay presented that the apoptosis rate of T47D and MDA-MB-231 cells transfected with si-MAFG-AS1#3 was markedly promoted compared with si-NC (**Figure 2G**). The protein levels of apoptosis-related markers (Bax and Bcl-2) were detected, and we found that the level of Bax was enhanced, while the level of Bcl-2 was weakened in T47D and MDA-MB-231 cells transfected with si-MAFG-AS1#3 compared with si-NC (**Figure 2H** and **2I**). Moreover, the glycolysis was assessed, and the resultindicated that the levels of glucose consumption and lactate production were inhibited in T47D and MDA-MB-231 cells transfected with si-MAFG-AS1#3 (**Figure 2J** and **2K**). Additionally, the protein levels of glycolysis indicators (HK2 and LDHA) were quantified, and the result showed that the levels of HK2 and LDHA were significantly lowerin T47D and MDA-MB-231 cells transfected with si-MAFG-AS1#3 compared with si-NC (**Figure 2L-O**). These data indicated that MAFG-AS1 knockdown inhibited cell proliferation, colony formation, and glycolysis, but induced cell apoptosis in breast cancer cells.

MiR-3196 was a direct target of MAFG-AS1

Generally, lncRNA functions by acting as "miRNA sponge" [29]. Next, we predicted and identified the potential target miRNAs of MAFG-AS1. As shown in **Figure 3A**, miR-3196 was a target of MAFG-AS1 with specific binding sites by the prediction of starBase (http://starbase.sysu.edu.cn/). The dual-luciferase reporter assay confirmed their relationship and showed that miR-3196 overexpression notably reduced the luciferase activity in T47D and MDA-MB-231 transfected with MAFG-AS1-WT but not MAFG-AS1-MUT (**Figure 3B** and **3C**). Moreover, miR-3196 was downregulated in breast cancer tumor tissues compared with that in normal tissues (**Figure 3D**). Likewise, the expression of miR-3196 was also reducedin T47D and MDA-MB-231 cells relative to MCF-10A cells (**Figure 3E**). Additionally, the expression of miR-3196 was negatively correlated with MAFG-AS1 expression (**Figure 3F**). MAGF-AS1 knockdown significantly promoted the expression of miR-3196 in T47D and MDA-MB-231 cells (**Figure 3G**). The above data indicated that miR-3196 was a target of MAFG-AS1.

The inhibition of miR-3196 reversed the role of MAGF-AS1 knockdown

To ascertain whether MAFG-AS1 participated in breast cancer progression by regulating miR-3196, T47D and MDA-MB-AS1 cells were introduced with si-MAFG-AS1#3 or si-MAFG-AS1#3+anti-miR-3196, si-NC or si-MAFG-AS1#3+anti-miR-NC acting as the control. First, the inhibition efficiency of miR-3196 was checked, and we found that the expression of miR-3196 was significantly declined in T47D and MDA-MB-AS1 cells transfected with anti-miR-3196 (**Figure 4A**). Next, we noticed that the expression of miR-3196 was elevated by si-MAFG-AS1#3 but suppressed by si-MAFG-AS1#3+anti-miR-3196

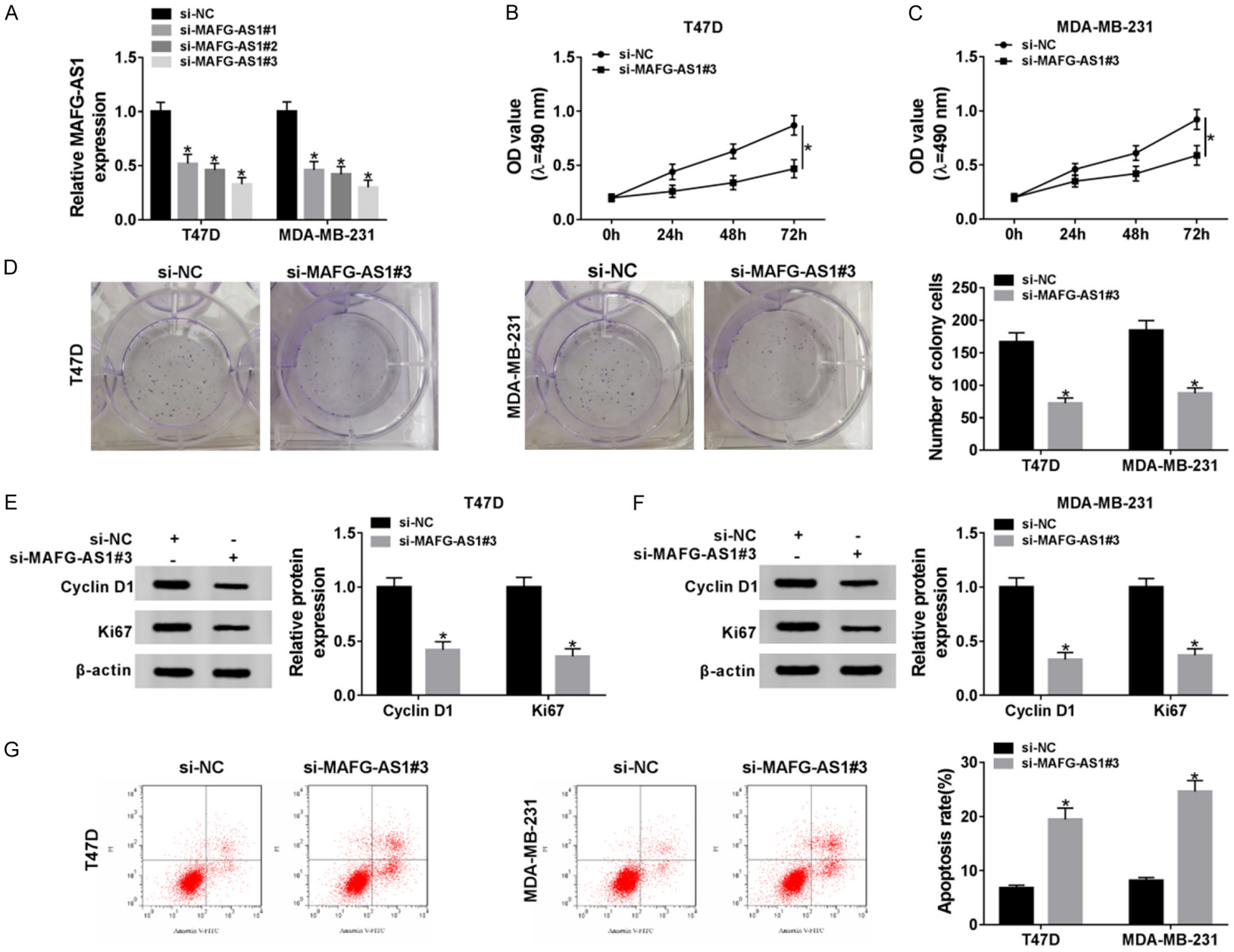
A
si-NC
si-MAFG-AS1#1
si-MAFG-AS1#2
si-MAFG-AS1#3
Relative MAFG-AS1 expression
T47D
MDA-MB-231
B
T47D
si-NC
si-MAFG-AS1#3
OD value (λ=490 nm)
0h
24h
48h
72h
C
MDA-MB-231
si-NC
si-MAFG-AS1#3
OD value (λ=490 nm)
0h
24h
48h
72h
D
si-NC
si-MAFG-AS1#3
T47D
MDA-MB-231
Number of colony cells
T47D
MDA-MB-231
E
si-NC
si-MAFG-AS1#3
Cyclin D1
Ki67
β-actin
T47D
Relative protein expression
Cyclin D1
Ki67
F
MDA-MB-231
G
Apoptosis rate(%)
T47D
MDA-MB-231

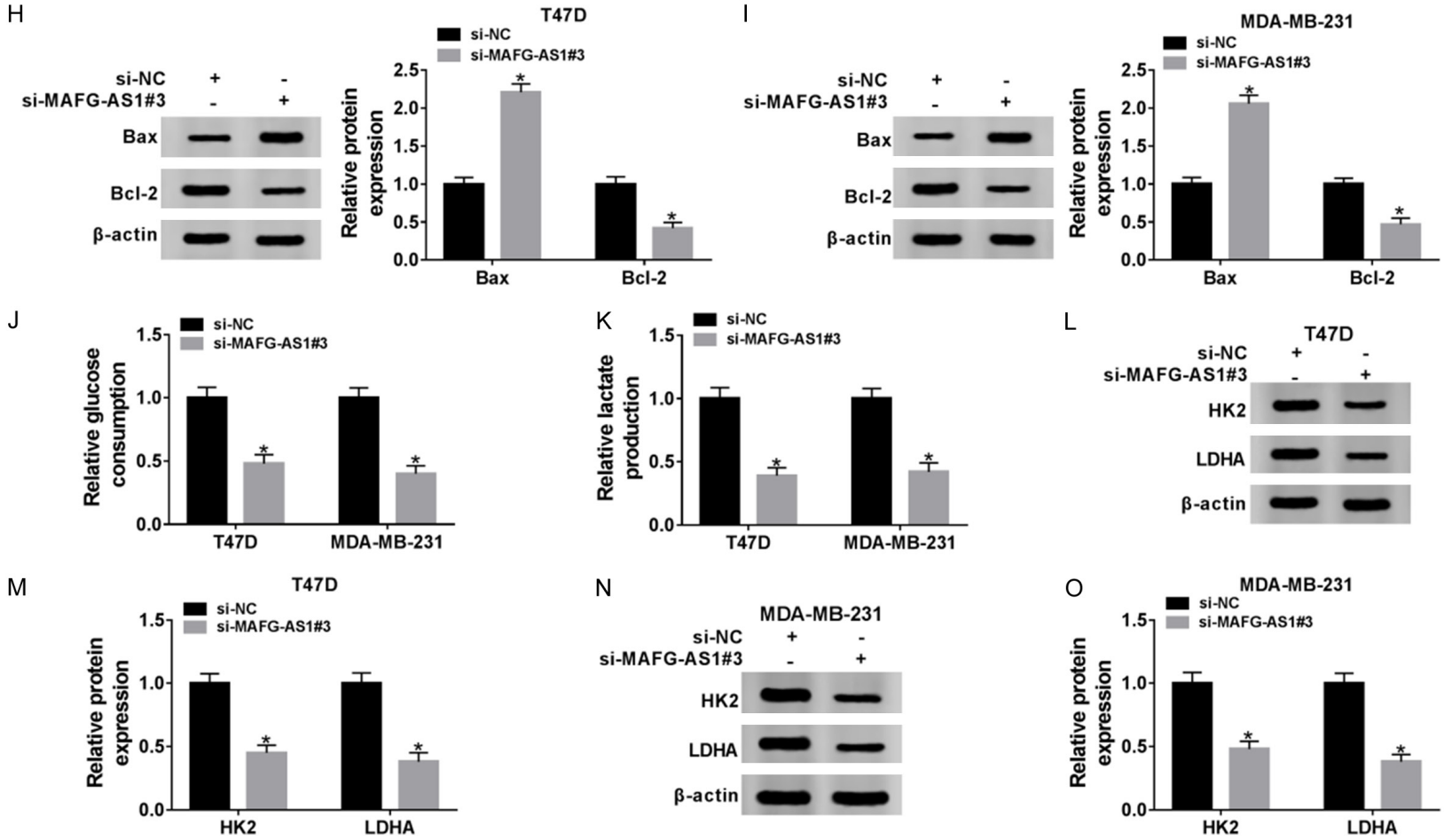

Figure 2. MAFG-AS1 knockdown inhibited cell proliferation, colony formation, and glycolysis but induced cell apoptosis. The endogenous level of MAFG-AS1 was knocked down by RNA interference in T470 and MDA-MB-231 cells. A. The interference efficiency of MAFG-AS1 was ascertained by qRT-PCR. B and C. The cell proliferation was assessed by MTT assay. D. The number of colonies was examined through colony formation assay. E and F. The levels of Cyclin D1 and Ki67 were quantified by western blot. G. Cell apoptosis was evaluated by flow cytometry. H and I. The levels of Bax and Bcl-2 were detected by western blot. J and K. The glycolysis progression was estimated through the levels of glucose consumption and lactate production. L-O. The levels of HK2 and LDHA were quantified by western blot. *$P < 0.05$.

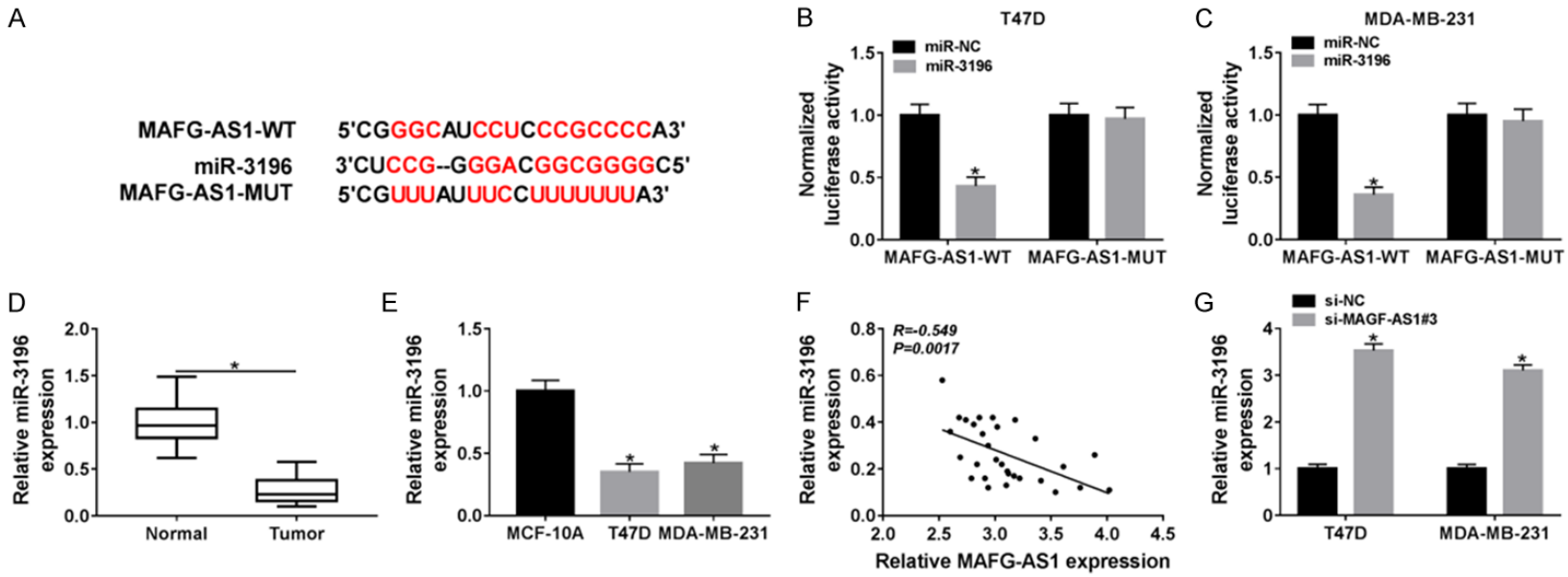

Figure 3. miR-3196 is a target of MAFG-AS1. A. The relationship between miR-3196 and MAFG-AS1 was predicted by the online tool starBase. B and C. The relationship between them was confirmed by dual-luciferase reporter assay. D and E. The expression of miR-3196 in breast tumor tissues and cell lines was checked by qRT-PCR. F. Spearman correlation analysis revealed a correlation between miR-3196 expression and MAFG-AS1 expression. G. The expression of miR-3196 in cells transfected with si-MAFG-AS1 or si-NC was detected by qRT-PCR. $*P < 0.05$.

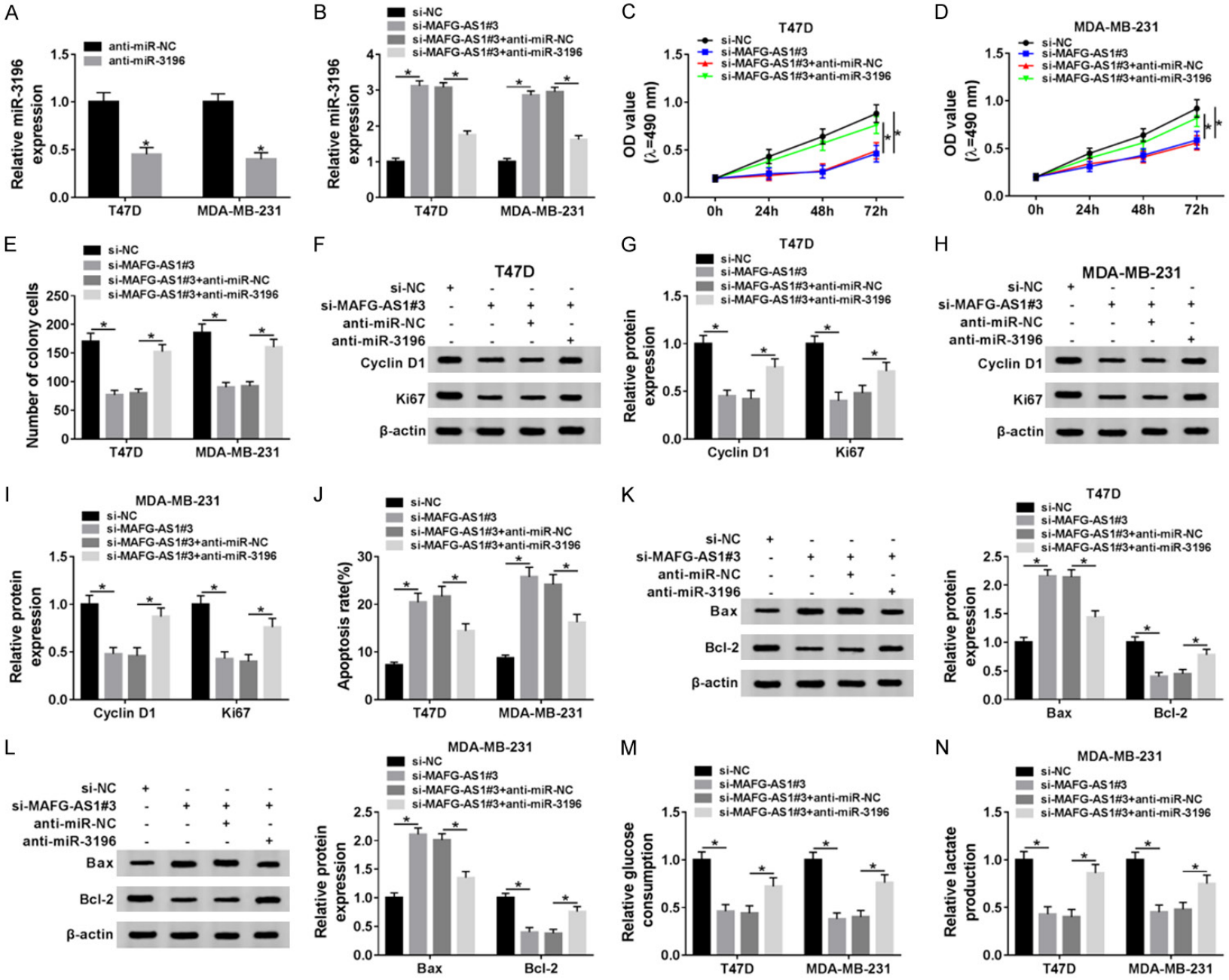
A
anti-miR-NC
anti-miR-3196
Relative miR-3196 expression
T47D
MDA-MB-231
B
si-NC
si-MAFG-AS1#3
si-MAFG-AS1#3+anti-miR-NC
si-MAFG-AS1#3+anti-miR-3196
Relative miR-3196 expression
T47D
MDA-MB-231
C
T47D
si-NC
si-MAFG-AS1#3
si-MAFG-AS1#3+anti-miR-NC
si-MAFG-AS1#3+anti-miR-3196
OD value (λ=490 nm)
0h
24h
48h
72h
D
MDA-MB-231
si-NC
si-MAFG-AS1#3
si-MAFG-AS1#3+anti-miR-NC
si-MAFG-AS1#3+anti-miR-3196
OD value (λ=490 nm)
0h
24h
48h
72h
E
si-NC
si-MAFG-AS1#3
si-MAFG-AS1#3+anti-miR-NC
si-MAFG-AS1#3+anti-miR-3196
Number of colony cells
T47D
MDA-MB-231
F
T47D
si-NC
si-MAFG-AS1#3
anti-miR-NC
anti-miR-3196
Cyclin D1
Ki67
β-actin
G
T47D
si-NC
si-MAFG-AS1#3
si-MAFG-AS1#3+anti-miR-NC
si-MAFG-AS1#3+anti-miR-3196
Relative protein expression
Cyclin D1
Ki67
H
MDA-MB-231
si-NC
si-MAFG-AS1#3
anti-miR-NC
anti-miR-3196
Cyclin D1
Ki67
β-actin
I
MDA-MB-231
si-NC
si-MAFG-AS1#3
si-MAFG-AS1#3+anti-miR-NC
si-MAFG-AS1#3+anti-miR-3196
Relative protein expression
Cyclin D1
Ki67
J
si-NC
si-MAFG-AS1#3
si-MAFG-AS1#3+anti-miR-NC
si-MAFG-AS1#3+anti-miR-3196
Apoptosis rate(%)
T47D
MDA-MB-231
K
si-NC
si-MAFG-AS1#3
anti-miR-NC
anti-miR-3196
Bax
Bcl-2
β-actin
T47D
si-NC
si-MAFG-AS1#3
si-MAFG-AS1#3+anti-miR-NC
si-MAFG-AS1#3+anti-miR-3196
Relative protein expression
Bax
Bcl-2
L
si-NC
si-MAFG-AS1#3
anti-miR-NC
anti-miR-3196
Bax
Bcl-2
β-actin
MDA-MB-231
si-NC
si-MAFG-AS1#3
si-MAFG-AS1#3+anti-miR-NC
si-MAFG-AS1#3+anti-miR-3196
Relative protein expression
Bax
Bcl-2
M
si-NC
si-MAFG-AS1#3
si-MAFG-AS1#3+anti-miR-NC
si-MAFG-AS1#3+anti-miR-3196
Relative glucose consumption
T47D
MDA-MB-231
N
MDA-MB-231
si-NC
si-MAFG-AS1#3
si-MAFG-AS1#3+anti-miR-NC
si-MAFG-AS1#3+anti-miR-3196
Relative lactate production
T47D
MDA-MB-231

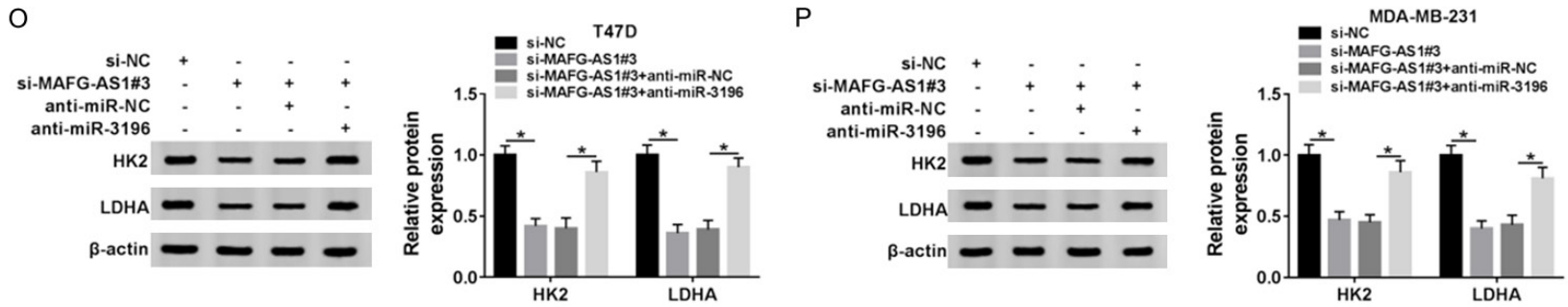

Figure 4. The inhibition of miR-3196 abolishes the effects of MAFG-AS1 knockdown. T470 and MDA-MB-231 cells were transfected with si-MAFG-AS1#3 or si-MAFG-AS1#3+anti-miR-3196, si-NC or si-MAFG-AS1#3+anti-miR-NC acting as the control, respectively. A. The inhibition efficiency of miR-3196 was determined by qRT-PCR. B. The transfection efficiency was examined by qRT-PCR. C and D. The cell proliferation was assessed by MTT assay. E. The number of colonies was examined through colony formation assay. F-I. The levels of Cyclin D1 and Ki67 were quantified by western blot. J. The cell apoptosis was evaluated by flow cytometry. K and L. The levels of Bax and Bcl-2 were detected by western blot. M and N. Glycolysis progression was estimated through the levels of glucose consumption and lactate production. O and P. The levels of HK2 and LDHA were quantified by western blot. $*P < 0.05$.

(**Figure 4B**). The cell proliferation that was inhibited in T47D and MDA-MB-AS1 cells transfected with si-MAFG-AS1#3 was promoted by si-MAFG-AS1#3+anti-miR-3196 transfection (**Figure 4C** and **4D**). The number of colonies was reduced by MAFG-AS1 knockdown but recovered by miR-3196 inhibition in T47D and MDA-MB-AS1 cells (**Figure 4E**). The protein levels of Cyclin D1 and Ki67 were depleted by MAFG-AS1 but restored by the combination of MAFG-AS1 knockdown and miR-3196 inhibition (**Figure 4F-I**). The apoptosis rate stimulated in cells transfected with si-MAFG-AS1#3 was blocked in cells with si-MAFG-AS1#3+anti-miR-3196 transfection (**Figure 4J**). The protein level of Bax was promoted by MAFG-AS1 knockdown but restrained by miR-3196 inhibition in T47D and MDA-MB-AS1 cells, while the level of Bcl-2 was opposite to Bax expression (**Figure 4K** and **4L**). The glucose consumption and lactate production that were inhibited in T47D and MDA-MB-AS1 cells transfected with si-MAFG-AS1#3, were rescued in cells with si-MAFG-AS1#3+anti-miR-3196 transfection (**Figure 4M** and **4N**). The protein levels of HK2 and LDHA were reducedin T47D and MDA-MB-AS1 cells transfected with si-MAFG-AS1#3 but recovered by si-MAFG-AS1#3+anti-miR-3196 transfection (**Figure 4O** and **4P**). The above data proved that MAFG-AS1 knockdown inhibited breast cancer malignant progression by enhancing the expression of miR-3196.

TFAP2A was a target of miR-3196

Given that miRNAs function by binding to the 3'UTR of target mRNAs, we predicted and analyzed the target mRNAs of miR-3196. As displayed in **Figure 5A**, TFAP2A was predicted as a target of miR-3196 with specific binding sites using the online tool starBase. Then, dual-luciferase reporter assay exhibited that miR-3196 reintroduction notably decreased the luciferase activity in T47D and MDA-MB-231 cells transfected with TFAP2A 3'UTR-WT but not TFAP2A 3'UTR-MUT (**Figure 5B** and **5C**). Subsequently, we found that the expression of TFAP2A at both mRNA and protein levels was abnormally elevated in breast cancer tissues relative to normal tissues (**Figure 5D** and **5E**). Similarly, the expression of TFAP2A at both mRNA and protein levels was also reinforced in T47D and MDA-MB-231 cells compared with that in MCF-10A cells (**Figure 5F** and **5G**). Moreover, the expression of TFAP2A was negatively correlated with miR-3196 expression but positively correlated with MAFG-AS1 expression in breast cancer tissues (**Figure 5H** and **5I**). Furthermore, the expression of miR-3196 was significantly strengthened in T47D and MDA-MB-231 cells transfected with miR-3196 relative to miR-NC (**Figure 5J**), but the expression of TFAP2A at both mRNA and protein levels was rapidly decreased (**Figure 5K** and **5L**). Conversely, the expression of TFAP2A at both mRNA and protein levels was notably enhanced in T47D and MDA-MB-231 cells transfected with pcDNA-TFAP2A compared with pcDNA (**Figure 5M** and **5N**). These analyses ensured that miR-3196 directly bound to TFAP2A and modulated the expression of TFAP2A.

TFAP2A overexpression abolished the role of miR-3196 reintroduction

T47D and MDA-MB-231 cells were introduced with miR-3196 or miR-3196+pcDNA-TFAP2A, respectively, miR-NC or miR-3196+pcDNA as the control. The transfection efficiency was determined at first, and the result showed that the expression of TFAP2A was reducedwith miR-3196 transfection relative to miR-NC but restored with miR-3196+pcDNA-TFAP2A transfection relative to miR-3196+pcDNA at both mRNA and protein levels (**Figure 6A** and **6B**). Then, the cell proliferation was inhibited by miR-3196 transfection but recovered by miR-3196+pcDNA-TFAP2A transfection (**Figure 6C** and **6D**). The number of colonies was depleted in T47D and MDA-MB-231 cells transfected with miR-3196, but was abrogated in cells transfected with miR-3196+pcDNA-TFAP2A (**Figure 6E**). The protein levels of Cyclin D1 and Ki67 were inhibited by miR-3196 reintroduction but promoted by the combination of miR-3196 reintroduction and TFAP2A overexpression (**Figure 6F** and **6G**). Moreover, the apoptosis rate was elevated in T47D and MDA-MB-231 cells transfected with miR-3196 but repressed with miR-3196+pcDNA-TFAP2A transfection (**Figure 6H**). The protein level of Bax was promoted in T47D and MDA-MB-231 cells transfected with miR-3196 but hampered with miR-3196+pcDNA-TFAP2A transfection, while the level of Bcl-2 was opposite to Bax expression (**Figure 6I-L**). Furthermore, the levels of glucose consump-

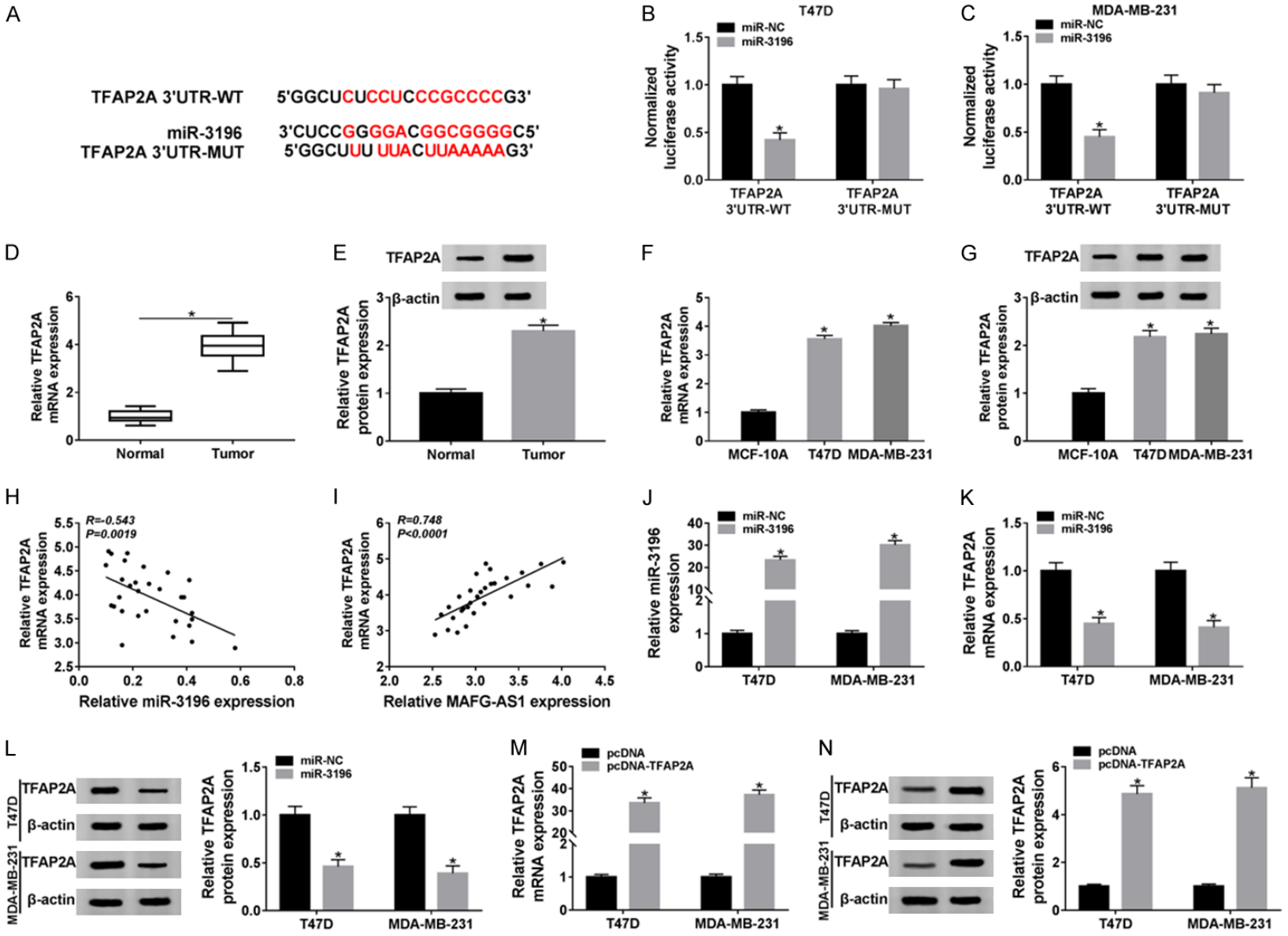
A
TFAP2A 3'UTR-WT
5'GGCUCUCCUCCCGCCCCG3'
miR-3196
3'CUCCGGGGACGGCGGGGC5'
TFAP2A 3'UTR-MUT
5'GGCUUU UUACUUAAAAAG3'
B
T47D
miR-NC
miR-3196
Normalized luciferase activity
TFAP2A 3'UTR-WT
TFAP2A 3'UTR-MUT
C
MDA-MB-231
miR-NC
miR-3196
Normalized luciferase activity
TFAP2A 3'UTR-WT
TFAP2A 3'UTR-MUT
D
Relative TFAP2A mRNA expression
Normal
Tumor
E
TFAP2A
β-actin
Relative TFAP2A protein expression
Normal
Tumor
F
Relative TFAP2A mRNA expression
MCF-10A
T47D
MDA-MB-231
G
TFAP2A
β-actin
Relative TFAP2A protein expression
MCF-10A
T47D
MDA-MB-231
H
R=-0.543
P=0.0019
Relative TFAP2A mRNA expression
Relative miR-3196 expression
I
R=0.748
P<0.0001
Relative TFAP2A mRNA expression
Relative MAFG-AS1 expression
J
miR-NC
miR-3196
Relative miR-3196 expression
T47D
MDA-MB-231
K
miR-NC
miR-3196
Relative TFAP2A mRNA expression
T47D
MDA-MB-231
L
T47D
TFAP2A
β-actin
MDA-MB-231
TFAP2A
β-actin
miR-NC
miR-3196
Relative TFAP2A protein expression
T47D
MDA-MB-231
M
pcDNA
pcDNA-TFAP2A
Relative TFAP2A mRNA expression
T47D
MDA-MB-231
N
T47D
TFAP2A
β-actin
MDA-MB-231
TFAP2A
β-actin
pcDNA
pcDNA-TFAP2A
Relative TFAP2A protein expression
T47D
MDA-MB-231

Figure 5. TFAP2A was a target of miR-3196. A. The relationship between miR-3196 and TFAP2A was predicted by the online tool starBase. B and C. The relationship between miR-3196 and TFAP2A was verified by dual-luciferase reporter assay. D and E. The expression of TFAP2A in breast tumor tissues was checked by qRT-PCR and western blot at both mRNA and protein levels. F and G. The expression of TFAP2A in breast cancer cell lines was checked by qRT-PCR and western blot at both mRNA and protein levels. H and I. Spearman correlation analysis revealed acorrelation between TFAP2A expression and miR-3196 expression or MAFG-AS1 expression in tumor tissues. J. The expression of miR-3196 was examined in T47D and MDA-MB-231 transfected with miR-3196 or miR-NC. K and L. The expression of TFAP2A was examined in T47D and MDA-MB-231 transfected with miR-3196 or miR-NC at both mRNA and protein levels. M and N. The expression of TFAP2A was examined in T47D and MDA-MB-231 transfected with pcDNA-TFAP2A or pcDNA at both mRNA and protein levels. *$P < 0.05$.

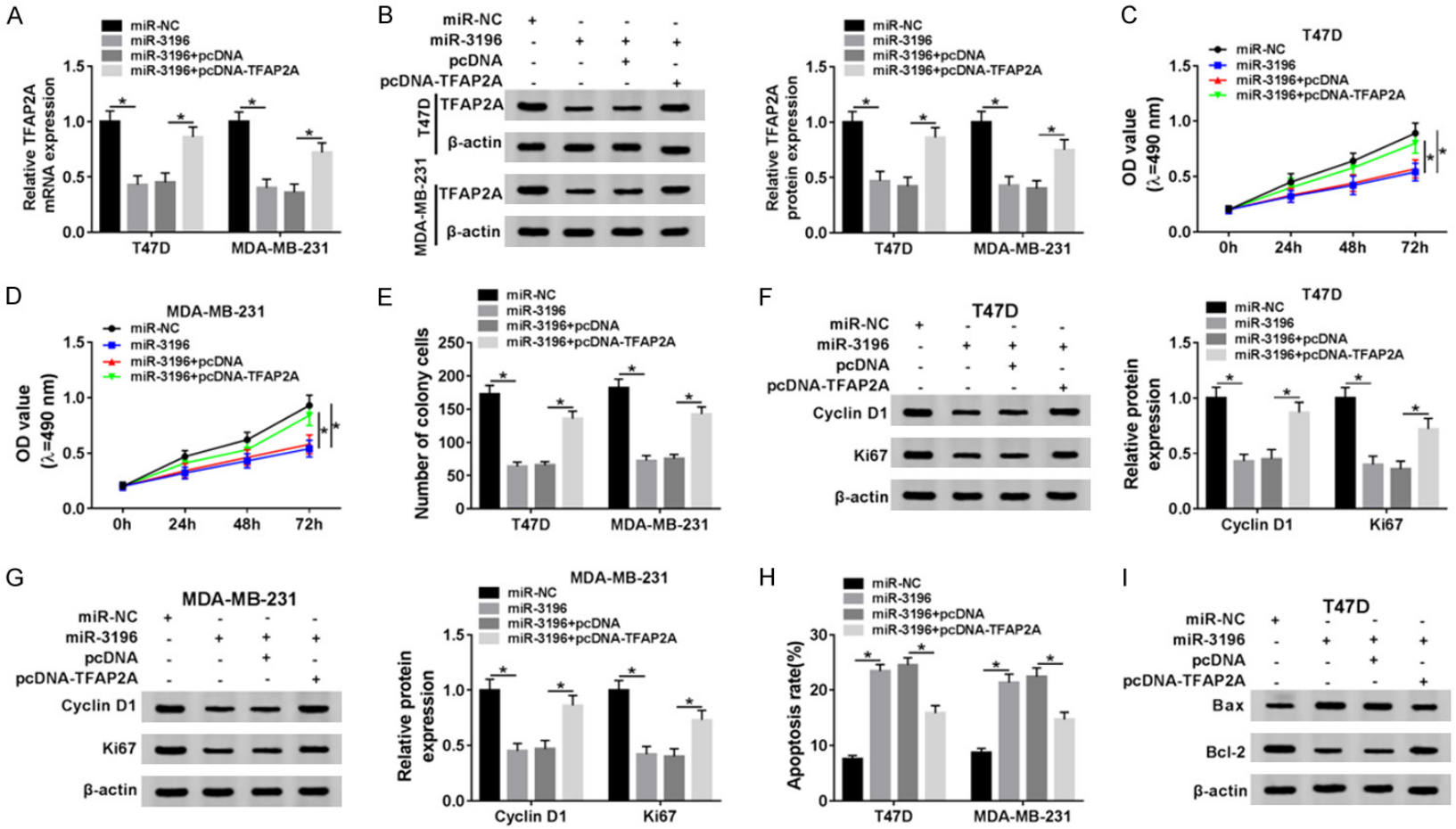

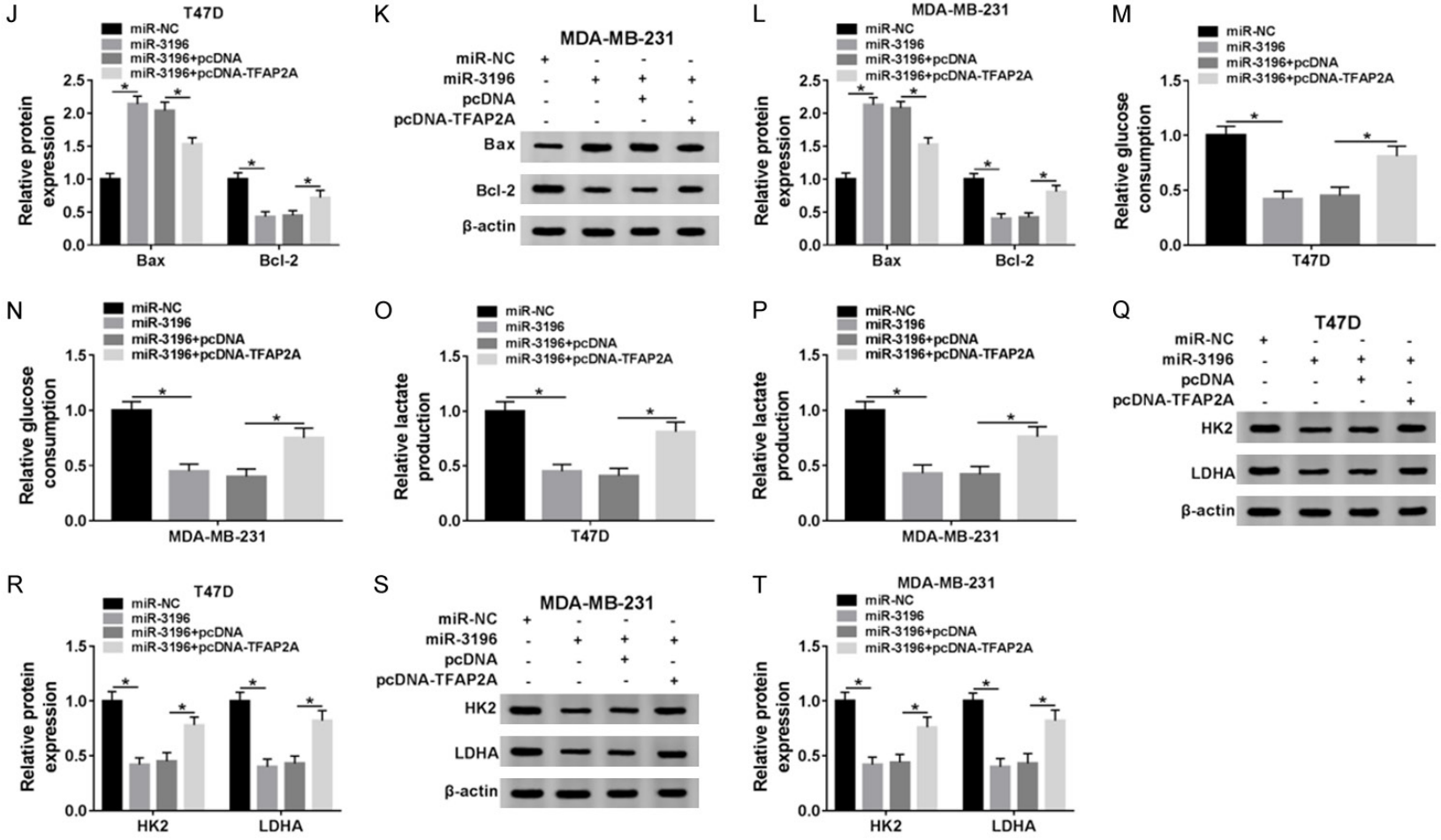

Figure 6. TFAP2A overexpression reversed the role of miR-3196 reintroduction. T47D and MDA-MB-231 cells were transfected with miR-3196 or miR-3196+pcDNA-TFAP2A, miR-NC or miR-3196+pcDNA acting as the controls, respectively. A and B. The expression of TFAP2A at both mRNA and protein levels was detected. C and D. The cell proliferation was assessed by MTT assay. E. The number of colonies was examined through colony formation assay. F and G. The levels of Cyclin D1 and Ki67 were quantified by western blot. H. The cell apoptosis was evaluated by flow cytometry. I-L. The levels of Bax and Bcl-2 were detected by western blot. M-P. Glycolysis progression was estimated through the levels of glucose consumption and lactate production. Q-T. The levels of HK2 and LDHA were quantified by western blot. *$P < 0.05$.

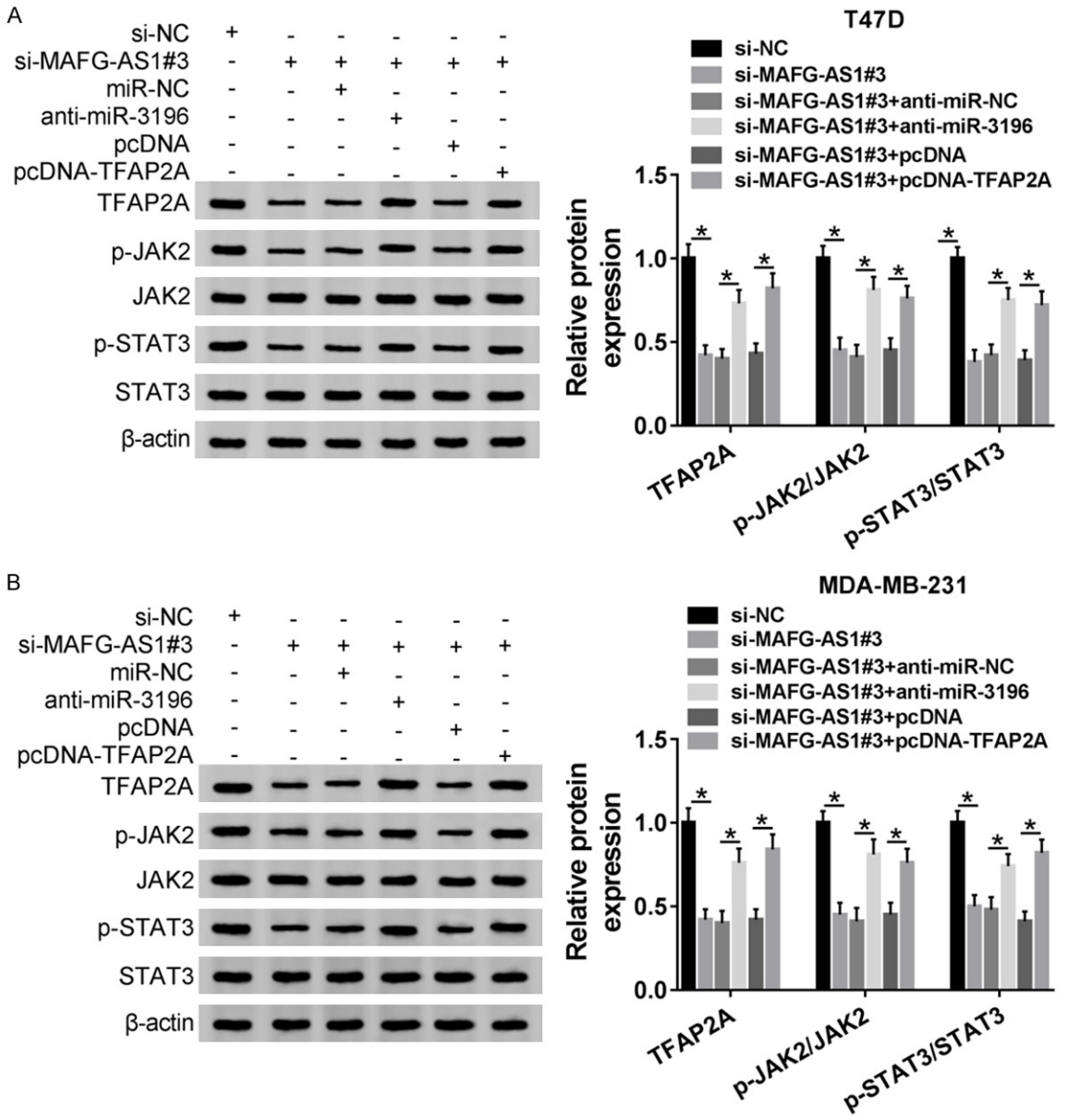

Figure 7. JAK2/STAT3 signaling pathway is involved in the MAFG-AS1/miR-3196/TFAP2A regulatory axis. T47D and MDA-MB-231 cells were transfected with si-MAFG-AS1#3, si-MAFG-AS1#3+anti-miR-3196 or si-MAFG-AS1#3+pcDNA-TFAP2A, si-NC, si-MAFG-AS1#3+anti-miR-NC or si-MAFG-AS1#3+pcDNA acting as the control, respectively. A and B. The relative protein levels of TFAP2A, p-JAK2/JAK2 and p-STAT3/STAT3 were measured by western blot. $*P < 0.05$.

tion and lactate production were restrained in T47D and MDA-MB-231 cells with miR-3196 reintroduction but regained by TFAP2A overexpression (**Figure 6M-P**). The protein levels of HK2 and LDHA were also impeded in cells with miR-3196 transfection but stimulated in cells with miR-3196+pcDNA-TFAP2A transfection (**Figure 6Q-T**). Collectively, miR-3196 reintroduction suppressed the malignant progression of breast cancer cells, which was reversed by TFAP2A overexpression.

MAFG-AS1 knockdown inactivated the JAK2/STAT3 signaling pathway through downregulating TFAP2A by upregulating miR-3196

To ascertain whether MAFG-AS1 exerted its role through modulating signaling pathways, we examined several the change of proteins on the pathway in T47D and MDA-MB-231 cells transfected with si-MAFG-AS1#3, si-MAFG-AS1#3+anti-miR-3196 or si-MAFG-AS1#3+pcDNA-TFAP2A, si-NC, si-MAFG-AS1#3+anti-miR-NC or si-

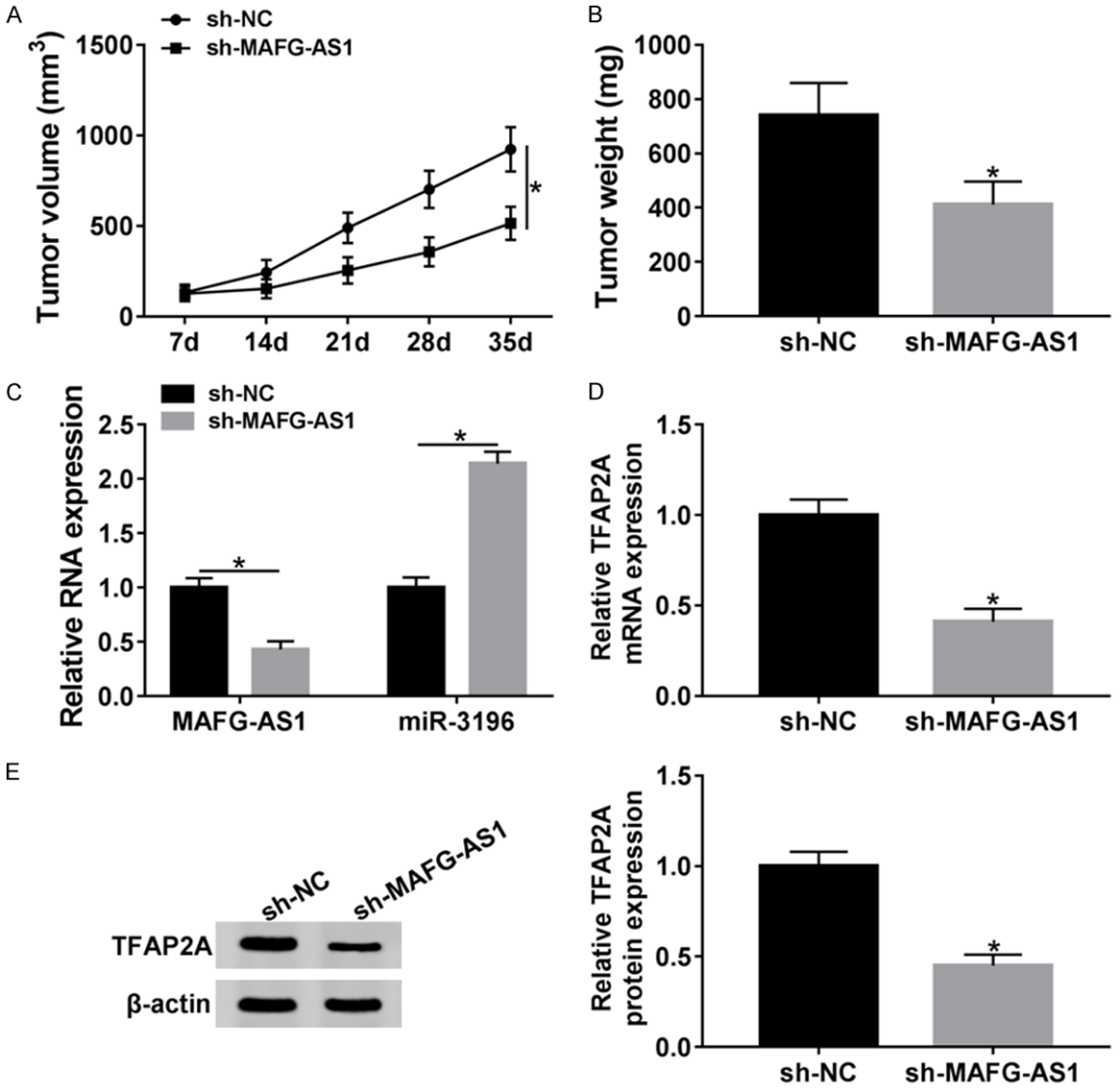

Figure 8. MAFG-AS1 knockdown suppresses tumor growth *in vivo*. A. The tumor volume was recorded once a week after injection. B. The tumor weight was measured after 35 days. C. The expression of MAFG-AS1 and miR-3196 in excised tumor tissues was detected by qRT-PCR. D and E. The expression of TFAP2A was examined in excised tumor tissues was detected by qRT-PCR and western blot at both mRNA and protein levels. *$P < 0.05$.

MAFG-AS1#3+pcDNA acting as the control, respectively. It was observed that the protein level of TFAP2A was significantly decreased in cells transfected with si-MAFG-AS1#3 but recovered in cells with si-MAFG-AS1#3+anti-miR-3196 or si-MAFG-AS1#3+pcDNA-TFAP2A transfection. The relative levels of p-JAK2/JAK2 and p-STAT3/STAT3 were weakened in T47D and MDA-MB-231 cells transfected with si-MAFG-AS1#3 but restored in cells transfected with si-MAFG-AS1#3+anti-miR-3196 or si-MAFG-AS1#3+pcDNA-TFAP2A (**Figure 7A** and **7B**), suggesting that MAFG-AS1 knockdown inactivated the JAK2/STAT2 pathway, while miR-3196 inhibition or TFAP2A overexpression re-activated the JAK2/STAT2 pathway.

MAFG-AS1 knockdown inhibited the tumor growth in vivo

Tumor formation assay in nude mice was performed to determine the role of MAFG-AS1 *in vivo*. As shown in **Figure 8A** and **8B**, MAFG-AS1 knockdown markedly reduced the tumor volume and tumor weight. qRT-PCR analysis exhibited that the expression of MAFG-AS1 was notably decreased in excised tumor tissues, while the expression of miR-3196 was strengthened

(**Figure 8C**). Moreover, the expression of TFAP-2A was significantly reducedin excised tumor tissues at both mRNA and protein levels (**Figure 8D** and **8E**). The data clarified that MAFG-AS1 knockdown restrained tumor growth *in vivo*.

Discussion

Breast cancer accounts for 12.2% of all cancer cases in Chinese women and 9.6% of all cancer-related deaths worldwide [7]. Breast cancer remains a central burden to women's lives. Therefore, it is essential to expound the underlying molecular mechanisms and pathogenesis associated with the tumorigenesis of breast cancer. The results from our present study manifested that MAFG-AS1 was upregulated in breast cancer tissues and cells. MAFG-AS1 knockdown inhibited proliferation, colony formation, and glycolysis but induced apoptosis of breast cancer cells. MiR-3196 was verified as a target of MAFG-AS1, and its inhibition reversed the role of MAFG-AS1 knockdown. TFAP2A was a target of miR-3196, and TFAP2A overexpression abolished the effects of miR-3196 reintroduction. Moreover, we found that MAFG-AS1 knockdown inactivated the JAK2/STAT3 signaling pathway. Additionally, MAFG-AS1 knockdown suppressed tumor growth *in vivo*. Our research revealed a new mechanism inbreast cancer.

Previous studies had reported the role of MAFG-AS1 in different cancers and related mechanisms. For example, Ouyang *et al.* observed that MAFG-AS1 contributed to proliferation, migration, and invasion by interacting with miR-6852 in hepatocellular carcinoma [19]. Cui *et al.* demonstrated that MAFG-AS1 overexpression accelerated the progression of colorectal cancer through the increase of cell proliferation, invasion, and glycolysis, and a decrease in cell apoptosis, which was accomplished by sponging miR-147b [4]. Interestingly, Li *et al.* illustrated that MAFG-AS1 promoted the malignant progression of breast cancer through the regulation of miR-339-5p/MMP15 [13]. Among these cancers, MAFG-AS1 was aberrantly upregulated in cancer tissues and cells relative to normal tissues. Consistent with these previous studies, the expression of MAFG-AS1 was also reinforced in breast cancer tissues and cells in our study, and its knockdown restrained the malignant behaviors of breast cancer cells *in vitro* and tumor growth *in vivo*. These findings suggested a consistent role of MAFG-AS1 in different types of cancer, promoting tumor progression.

lncRNAs act as "sponges" toabsorb miRNAs, leading to the inhibition of expression of miRNAs [18]. Here, miR-3196 was confirmed as a target of MAFG-AS1. It had been reported that miR-3196 was downregulated in basal cell carcinoma, gastric cancer, and breast cancer [11, 12, 21], and the anti-tumor role of miR-3196 was preliminarily demonstrated in these cancers. Also, we noticed a reduced abundance of miR-3196 in breast cancer tissues and cells, and its reintroduction suppressed the aggressive progression of breast cancer cells. The classic mode of action of miRNAs is to interact with the target sites located in the 3'UTR of downstream mRNAs to modulate gene expression [9]. Here, the relationship between miR-3196 and TFAP2A was predicted by the online bioinformatics tool and verified by the dual-luciferase reporter assay. TFAP2A, acting as an oncogene, is implicated in numerous cancers, including breast cancer. A previous study stated that TFAP2A was richly expressed in breast cells MDA-MB-453 [34]. Another study insisted that miR-876-5p restrained cell proliferation, migration and invasion bybinding to TFAP2A [33]. In line with these findings, we discovered that TFAP2A was aberrantly upregulated in breast cancer tissues and cells, and its overexpression abolished the role of miR-3196 reintroduction, maintaining the carcinogenicity of TFAP2A in human cancers. Notably, the JAK2/STAT3 signaling pathway was concluded to be involved in the regulatory axis of MAFG-AS1 in breast cancer. The activation of the JAK2/STAT3 pathway was closely linked to the development of cancer. For instance, Basic transcription factor 3 exacerbated gastric cancer mainly through the stimulation of the JAK2/STAT3 signaling pathway [36]. LncRNA HOST2 downregulation benefited tthe suppression of cell migration and invasion through weakening the phosphorylation levels of JAK2 and STAT3 [32]. The data point out the vital role of the activation of JAK2/STAT3 pathway during the cancer progress. Similarly in our study, MAFG-AS1 knockdown led to the inactivation of the JAK2/STAT3 pathway to attenuate the progression of breast cancer.

Thus, MAFG-AS1 is abnormally upregulated in breast cancer tissues and cells. MAFG-AS1 knockdown altered cell proliferation and colony formation, triggered cell apoptosis, and blocked glycolysis through inactivating the JAK2/STAT3 signaling pathway by the MAFG-AS1/miR-3196/TFAP2A axis. Our research shows the functional role of MAFG-AS1 in breast cancer and the associated action mechanism, providing a promising therapeutic approach for breast cancer.

Acknowledgements

The present study was supported by grants from the Experimental Animal Science and Technology Project of Zhejiang Province, China (grant no. 2015C37088), and Science and Technology Project of Jinhua City in China (grants no. 2018-3-024).

Disclosure of conflict of interest

None.

Address correspondence to: Mingxing Ding, Medical Molecular Biology Laboratory, Medical College, Jinhua Polytechnic, 1188 Wuzhou Road, Jinhua 321017, Zhejiang, China. Tel: +86-0579-82265103; E-mail: mtd5tc@163.com

References

[1] Anastasiadou E, Jacob LS and Slack FJ. Non-coding RNA networks in cancer. Nat Rev Cancer 2018; 18: 5-18.

[2] Cerk S, Schwarzenbacher D, Adiprasito JB, Stotz M, Hutterer GC, Gerger A, Ling H, Calin GA and Pichler M. Current status of long non-coding rnas in human breast cancer. Int J Mol Sci 2016; 17.

[3] Croset M, Pantano F, Kan CWS, Bonnelye E, Descotes F, Alix-Panabieres C, Lecellier CH, Bachelier R, Allioli N, Hong SS, Bartkowiak K, Pantel K and Clezardin P. miRNA-30 family members inhibit breast cancer invasion, osteomimicry, and bone destruction by directly targeting multiple bone metastasis-associated genes. Cancer Res 2018; 78: 5259-5273.

[4] Cui S, Yang X, Zhang L, Zhao Y and Yan W. LncRNA MAFG-AS1 promotes the progression of colorectal cancer by sponging miR-147b and activation of NDUFA4. Biochem Biophys Res Commun 2018; 506: 251-258.

[5] Dimitrova Y, Gruber AJ, Mittal N, Ghosh S, Dimitriades B, Mathow D, Grandy WA, Christofori G and Zavolan M. TFAP2A is a component of the ZEB1/2 network that regulates TGFB1-induced epithelial to mesenchymal transition. Biol Direct 2017; 12: 8.

[6] Dong H, Wang W, Mo S, Chen R, Zou K, Han J, Zhang F and Hu J. SP1-induced lncRNA AGAP2-AS1 expression promotes chemoresistance of breast cancer by epigenetic regulation of MyD88. J Exp Clin Cancer Res 2018; 37: 202.

[7] Fan L, Strasser-Weippl K, Li JJ, St Louis J, Finkelstein DM, Yu KD, Chen WQ, Shao ZM and Goss PE. Breast cancer in China. Lancet Oncol 2014; 15: e279-289.

[8] Ferlay J, Soerjomataram I, Dikshit R, Eser S, Mathers C, Rebelo M, Parkin DM, Forman D and Bray F. Cancer incidence and mortality worldwide: sources, methods and major patterns in GLOBOCAN 2012. Int J Cancer 2015; 136: E359-386.

[9] Gu S, Jin L, Zhang F, Sarnow P and Kay MA. Biological basis for restriction of microRNA targets to the 3' untranslated region in mammalian mRNAs. Nat Struct Mol Biol 2009; 16: 144-150.

[10] Hayes EL and Lewis-Wambi JS. Mechanisms of endocrine resistance in breast cancer: an overview of the proposed roles of noncoding RNA. Breast Cancer Res 2015; 17: 40.

[11] Huang Z and Yang H. Upregulation of the long noncoding RNA ADPGK-AS1 promotes carcinogenesis and predicts poor prognosis in gastric cancer. Biochem Biophys Res Commun 2019; 513: 127-134.

[12] Ji ZC, Han SH and Xing YF. Overexpression of miR-3196 suppresses cell proliferation and induces cell apoptosis through targeting ERBB3 in breast cancer. Eur Rev Med Pharmacol Sci 2018; 22: 8383-8390.

[13] Li H, Zhang GY, Pan CH, Zhang XY and Su XY. LncRNA MAFG-AS1 promotes the aggressiveness of breast carcinoma through regulating miR-339-5p/MMP15. Eur Rev Med Pharmacol Sci 2019; 23: 2838-2846.

[14] Liang H, Ge F, Xu Y, Xiao J, Zhou Z, Liu R and Chen C. miR-153 inhibits the migration and the tube formation of endothelial cells by blocking the paracrine of angiopoietin 1 in breast cancer cells. Angiogenesis 2018; 21: 849-860.

[15] Lo PK, Wolfson B, Zhou X, Duru N, Gernapudi R and Zhou Q. Noncoding RNAs in breast cancer. Brief Funct Genomics 2016; 15: 200-221.

[16] Nordentoft I, Dyrskjot L, Bodker JS, Wild PJ, Hartmann A, Bertz S, Lehmann J, Orntoft TF and Birkenkamp-Demtroder K. Increased expression of transcription factor TFAP2alpha correlates with chemosensitivity in advanced bladder cancer. BMC Cancer 2011; 11: 135.

[17] O'Hara SP, Mott JL, Splinter PL, Gores GJ and LaRusso NF. MicroRNAs: key modulators of posttranscriptional gene expression. Gastroenterology 2009; 136: 17-25.

[18] Olgun G, Sahin O and Tastan O. Discovering lncRNA mediated sponge interactions in breast cancer molecular subtypes. BMC Genomics 2018; 19: 650.
[19] Ouyang H, Zhang L, Xie Z and Ma S. Long noncoding RNA MAFG-AS1 promotes proliferation, migration and invasion of hepatocellular carcinoma cells through downregulation of miR-6852. Exp Ther Med 2019; 18: 2547-2553.
[20] Perou CM, Sorlie T, Eisen MB, van de Rijn M, Jeffrey SS, Rees CA, Pollack JR, Ross DT, Johnsen H, Akslen LA, Fluge O, Pergamenschikov A, Williams C, Zhu SX, Lonning PE, Borresen-Dale AL, Brown PO and Botstein D. Molecular portraits of human breast tumours. Nature 2000; 406: 747-752.
[21] Sand M, Skrygan M, Sand D, Georgas D, Hahn SA, Gambichler T, Altmeyer P and Bechara FG. Expression of microRNAs in basal cell carcinoma. Br J Dermatol 2012; 167: 847-855.
[22] Santana-Davila R and Perez EA. Treatment options for patients with triple-negative breast cancer. J Hematol Oncol 2010; 3: 42.
[23] Schulte JH, Kirfel J, Lim S, Schramm A, Friedrichs N, Deubzer HE, Witt O, Eggert A and Buettner R. Transcription factor AP2alpha (TFAP2a) regulates differentiation and proliferation of neuroblastoma cells. Cancer Lett 2008; 271: 56-63.
[24] Schwarzenbacher D, Klec C, Pasculli B, Cerk S, Rinner B, Karbiener M, Ivan C, Barbano R, Ling H, Wulf-Goldenberg A, Stanzer S, Rinnerthaler G, Stoeger H, Bauernhofer T, Haybaeck J, Hoefler G, Jahn SW, Parrella P, Calin GA and Pichler M. MiR-1287-5p inhibits triple negative breast cancer growth by interaction with phosphoinositide 3-kinase CB, thereby sensitizing cells for PI3Kinase inhibitors. Breast Cancer Res 2019; 21: 20.
[25] Siegel RL, Miller KD and Jemal A. Cancer statistics, 2015. CA Cancer J Clin 2015; 65: 5-29.
[26] Tano K and Akimitsu N. Long non-coding RNAs in cancer progression. Front Genet 2012; 3: 219.
[27] Vennin C, Spruyt N, Robin YM, Chassat T, Le Bourhis X and Adriaenssens E. The long noncoding RNA 91H increases aggressive phenotype of breast cancer cells and up-regulates H19/IGF2 expression through epigenetic modifications. Cancer Lett 2017; 385: 198-206.
[28] Wang B, Li J, Sun M, Sun L and Zhang X. miRNA expression in breast cancer varies with lymph node metastasis and other clinicopathologic features. IUBMB Life 2014; 66: 371-377.
[29] Wang H, Niu L, Jiang S, Zhai J, Wang P, Kong F and Jin X. Comprehensive analysis of aberrantly expressed profiles of lncRNAs and miRNAs with associated ceRNA network in muscle-invasive bladder cancer. Oncotarget 2016; 7: 86174-86185.
[30] Wang MJ, Zhang H, Li J and Zhao HD. microRNA-98 inhibits the proliferation, invasion, migration and promotes apoptosis of breast cancer cells by binding to HMGA2. Biosci Rep 2018; 38.
[31] Wang W and Luo YP. MicroRNAs in breast cancer: oncogene and tumor suppressors with clinical potential. J Zhejiang Univ Sci B 2015; 16: 18-31.
[32] Wu Y, Yuan T, Wang WW, Ge PL, Gao ZQ, Zhang G, Tang Z, Dang XW, Zhao YF, Zhang JY and Jiang GZ. Long noncoding RNA HOST2 promotes epithelial-mesenchymal transition, proliferation, invasion and migration of hepatocellular carcinoma cells by activating the JAK2-STAT3 signaling pathway. Cell Physiol Biochem 2018; 51: 301-314.
[33] Xu J, Zheng J, Wang J and Shao J. miR-876-5p suppresses breast cancer progression through targeting TFAP2A. Exp Ther Med 2019; 18: 1458-1464.
[34] Yan F, He Q, Hu X, Li W, Wei K, Li L, Zhong Y, Ding X, Xiang S and Zhang J. Direct regulation of caspase3 by the transcription factor AP2alpha is involved in aspirininduced apoptosis in MDAMB453 breast cancer cells. Mol Med Rep 2013; 7: 909-914.
[35] Yeh CC, Luo JL, Nhut Phan N, Cheng YC, Chow LP, Tsai MH, Chuang EY and Lai LC. Different effects of long noncoding RNA NDRG1-OT1 fragments on NDRG1 transcription in breast cancer cells under hypoxia. RNA Biol 2018; 15: 1487-1498.
[36] Zhang DZ, Chen BH, Zhang LF, Cheng MK, Fang XJ and Wu XJ. Basic transcription factor 3 is required for proliferation and epithelial-mesenchymal transition via regulation of FOXM1 and JAK2/STAT3 signaling in gastric cancer. Oncol Res 2017; 25: 1453-1462.